Tagged Neutron DVCS with Bonus in CLAS12

R. Dupré, M. Ehrhart, M. Guidal, D. Marchand, C. Muñoz, S. Niccolai, E. Voutier

Institut de Physique Nucléaire, CNRS-IN2P3, Univ. Paris-Sud, Université Paris-Saclay, 91406 Orsay Cedex, France

a CLAS Collaboration Proposal

Abstract

The three-dimensional picture of quarks and gluons in the nucleon is set to be revealed through deeply virtual Compton scattering (DVCS). With the absence of a free neutron target, the deuterium target represents the simplest nucleus to be used to probe the internal 3D partonic structure of the quasi-free neutron. We propose to measure the beam spin asymmetry (BSA) in incoherent neutron DVCS together with the approved BONuS12 experiment, using the same beam time and are asking for the electron beam to be highly polarized. The DVCS BSA on a (quasi-free) neutron will be measured in a wide range of kinematics by tagging the scattered electron and the real photon final state with the spectator proton. We will also measure BSA with all final state particles detected; the scattered electron, the real photon, the spectator proton, and the struck neutron. Both measurements of BSA of neutron DVCS, by tagging the recoil proton and in the fully exclusive final state, will help to understand the impact of the final state interactions (FSI) and Fermi motion on the incoherent neutron DVCS. The proposed measurements are highly complementary to the approved CLAS12 experiment E12-11-003, which will also measure the quasi-free neutron DVCS by detecting the scattered neutron.

Contents

Introduction

Chapter 1

Tagged Neutron DVCS

Chapter to introduce the physics

1.1 First section

Chapter 2

Run conditions and Experimental setup

2.1 Run Group F

2.2 The CLAS12 Spectrometer

The CLAS12 detector is designed to operate with 11 GeV beam at an electron-nucleon luminosity of $\mathcal{L} = 1 \times 10^{35}$ cm^{-2}s^{-1}. The baseline configuration of the CLAS12 detector consists of the forward detector and the central detector packages [**?**] (see Figure 2.1). We use the forward detector for electron detection, while DVCS centered proposals also use it for photon detection. The central detector's silicon tracker and barrel micromegas will be removed to leave room for the BONuS12 RTPC.

The scattered electrons and photons will be detected in the forward detector which consists of the High Threshold Cherenkov Counters (HTCC), Drift Chambers (DC), the Low Threshold Cherenkov Counters (LTCC), the Time-of-Flight scintillators (TOF), the Forward Calorimeter and the Preshower Calorimeter. The charged particle identification in the forward detector is achieved by utilizing the combination of the HTCC, LTCC and TOF arrays with the tracking information from the Drift Chambers. The HTCC together with the Forward Calorimeter and the Preshower Calorimeter will provide a pion rejection factor of more than 2000 up to a momentum of 4.9 GeV/c, and a rejection factor of 100 above 4.9 GeV/c. The photons are detected using the calorimeters.

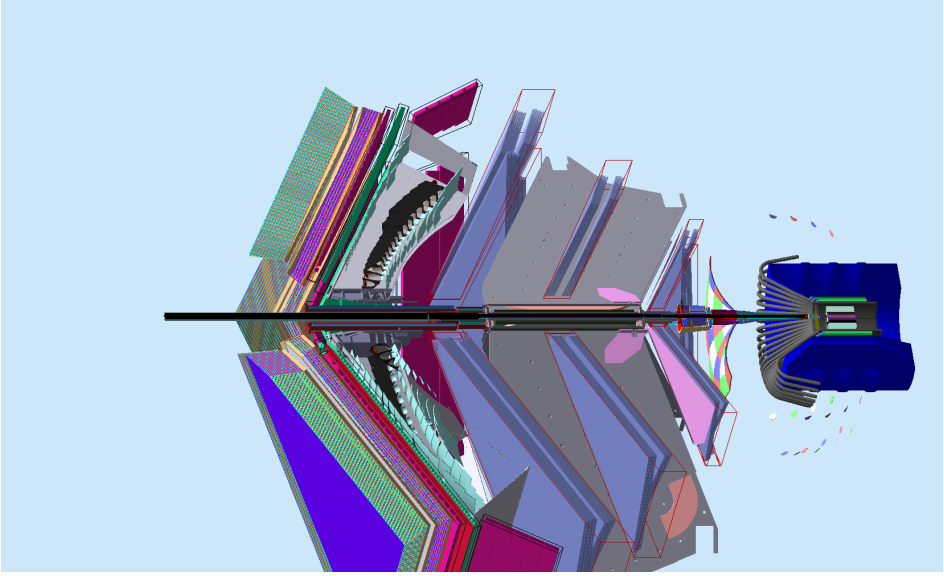

Figure 2.1: The schematic layout of the CLAS12 baseline design with BONuS12 RTPC replacing the silicon tracker and the barrel micromegas.

Chapter 3

Projections for the Proposed Measurements

3.1 Monte-Carlo Simulation

An event generator for DVCS/BH and exclusive π^0 electroproduction on the neutron inside a deuterium target has been developed [1]. The DVCS amplitude is calculated according to the BKM formalism [2], while the GPDs have been taken from the standard CLAS DVCS generator [3, 4]. The Fermi-motion distribution is calculated with the Paris potential [5].

The output of the event generator was fed through CLAS12 official simulation and reconstruction chain, to simulate the acceptance and resolutions of electrons and photons in the Forward Detector. Final state neutrons being detected in the central detector of CLAS12, and the final state recoiling protons in the BONuS12 RTPC.

Figure 3.1 shows the kinematic distributions of the DVCS electrons being detected and reconstructed in the forward detector of CLAS12 spectrometer in terms of the energy as a function of the polar angle (θ) and the azimuthal angle (ϕ) as a function of θ. Figure 3.4 presents the kinematic distributions of the neutron-DVCS photons detected in the CLAS12 forward detector.

3.4, and **??** show θ as a function of momentum in the lab frame and for, respectively, the electron, the photon and the neutron. The two panels of Fig. **??** are one-dimensional plots, showing, respectively, the momentum and the polar angle of the recoil neutron. As expected, the electron and the photon are mostly emitted at forward angles, while the recoil neutron is going at backwards angles.

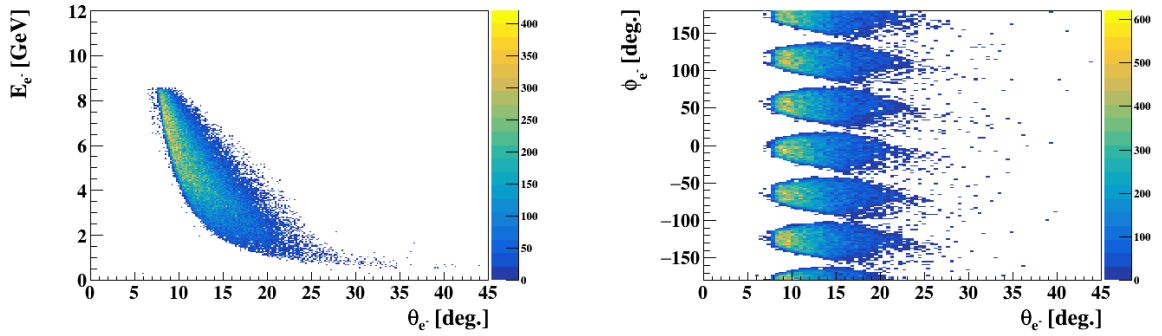

Figure 3.1: Electron's energy as a function of it's polar angle (left) and the azimuthal angle as a function of the polar angle (right), for n-DVCS events. Forward-CLAS12 acceptance and physics cuts are included.

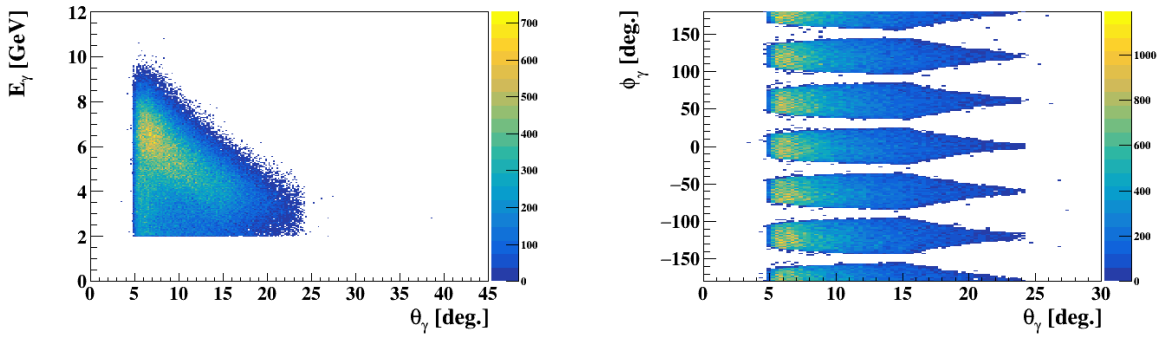

Figure 3.2: Photon's energy as a function of it's polar angle (left) and the azimuthal angle as a function of the polar angle (right), for n-DVCS events. Forward-CLAS12 acceptance and physics cuts are included.

3.2 Projections

3.2.1 Semi-exclusive selection

3.2.2 Semi-exclusive selection

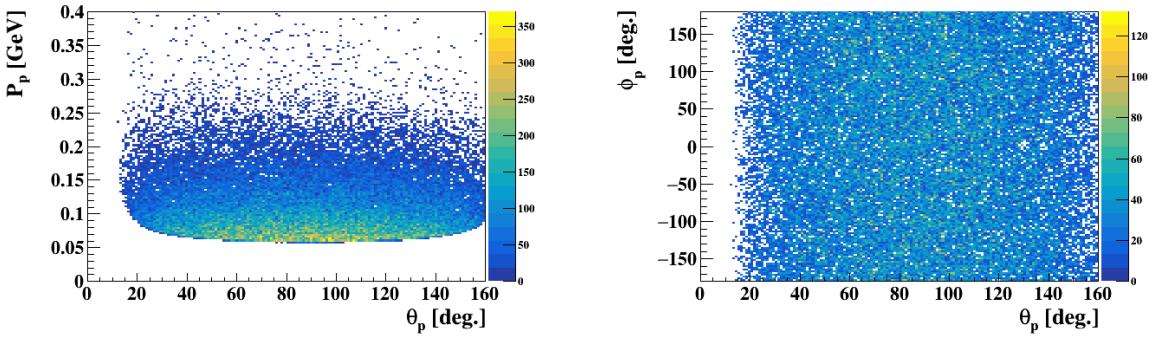

Figure 3.3: Recoiling proton's momentum as a function of it's polar angle (left) and the azimuthal angle as a function of the polar angle (right), from n-DVCS events. BONuS12 RTPC acceptance and physics cuts are included.

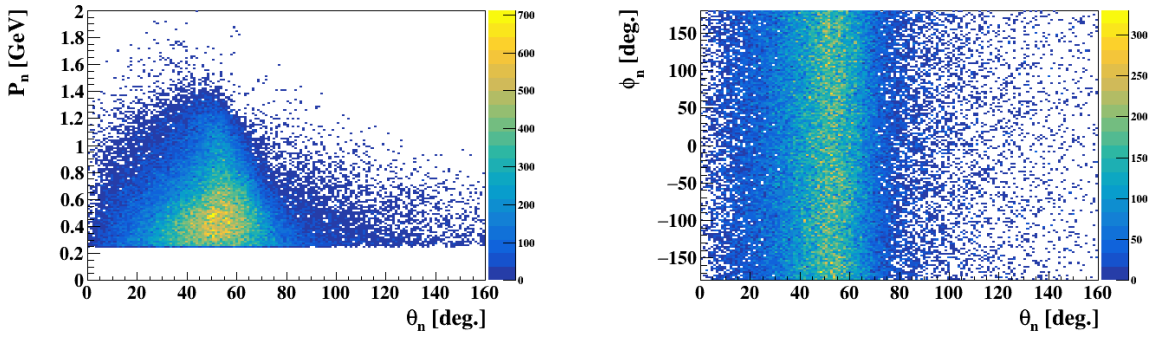

Figure 3.4: Recoiling neutron's momentum as a function of it's polar angle (left) and the azimuthal angle as a function of the polar angle (right), from n-DVCS events. BONuS12 RTPC acceptance and physics cuts are included.

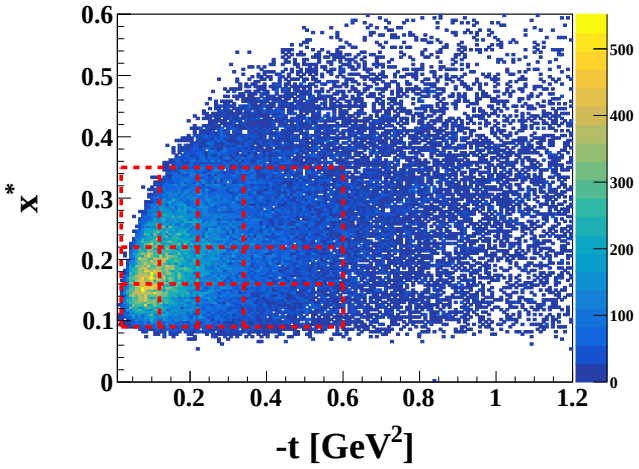

Figure 3.5: Data binning in x^* vs $-t$ space.

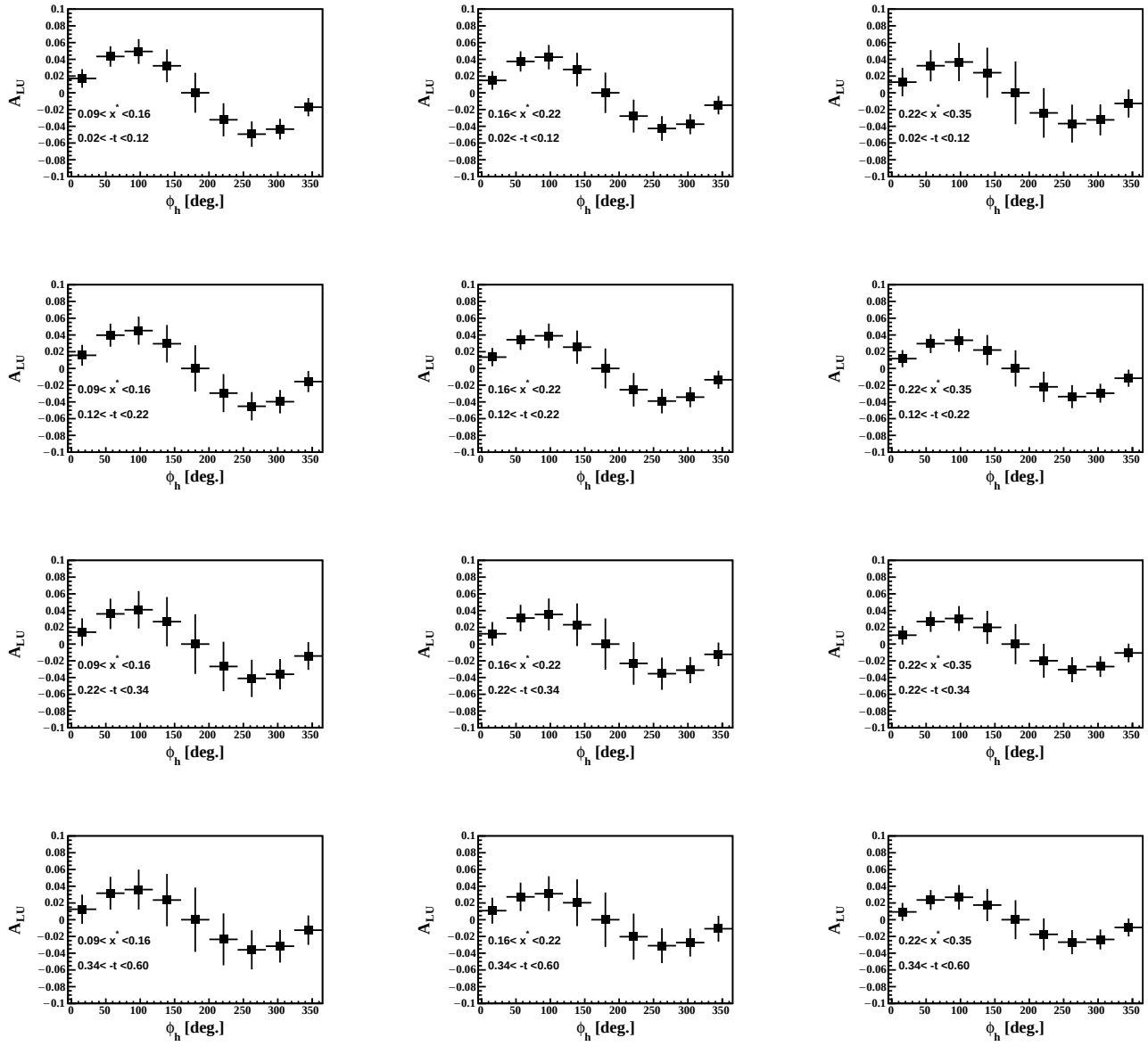

Figure 3.6: Projected beam-spin asymmetries as a function of the hadronic angle ϕ_h in the binning of x^* vs $-t$ space.

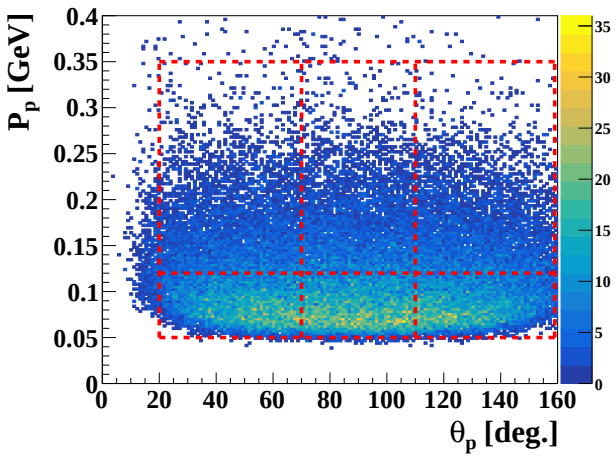

Figure 3.7: Data binning in p_s vs θ_s space.

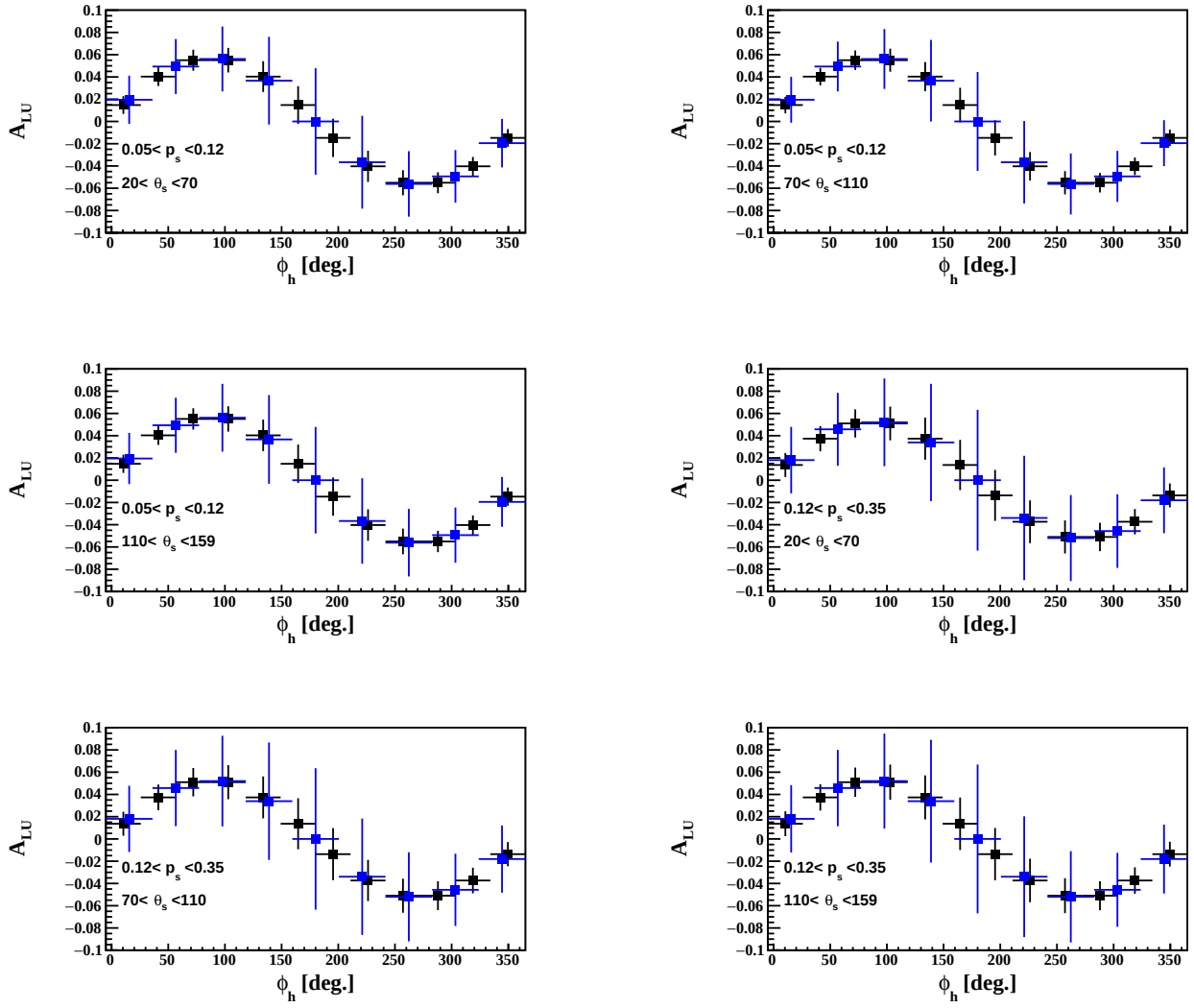

Figure 3.8: Projected beam-spin asymmetries as a function of the hadronic angle ϕ_h in the binning of p_s vs θ_s space.

Summary

Bibliography

[1] A. E. Alaoui and E. Voutier *CLAS Note 2009-024*.

[2] A. V. Belitsky, D. Mueller, and A. Kirchner, "Theory of deeply virtual Compton scattering on the nucleon," *Nucl. Phys.*, vol. B629, pp. 323–392, 2002.

[3] M. Vanderhaeghen, P. A. M. Guichon, and M. Guidal, "Deeply virtual electroproduction of photons and mesons on the nucleon: Leading order amplitudes and power corrections," *Phys. Rev. D*, vol. 60, p. 094017, Oct 1999.

[4] M. Guidal, M. V. Polyakov, A. V. Radyushkin, and M. Vanderhaeghen, "Nucleon form-factors from generalized parton distributions," *Phys. Rev.*, vol. D72, p. 054013, 2005.

[5] M. Lacombe, B. Loiseau, J. M. Richard, R. V. Mau, J. Côté, P. Pirès, and R. de Tourreil, "Parametrization of the paris $n - n$ potential," *Phys. Rev. C*, vol. 21, pp. 861–873, Mar 1980.